SOLAR NEUTRINOS REVIEW

Revised December 2007 by K. Nakamura (KEK, High Energy Accelerator Research Organization, Japan).

1. Introduction

The Sun is a main-sequence star at a stage of stable hydrogen burning. It produces an intense flux of electron neutrinos as a consequence of nuclear fusion reactions whose combined effect is

$$4p \rightarrow {}^4\mathrm{He} + 2e^+ + 2\nu_e. \qquad (1)$$

Positrons annihilate with electrons. Therefore, when considering the solar thermal energy generation, a relevant expression is

$$4p + 2e^- \rightarrow {}^4\mathrm{He} + 2\nu_e + 26.73\ \mathrm{MeV} - E_\nu\ , \qquad (2)$$

where E_ν represents the energy taken away by neutrinos, with an average value being $\langle E_\nu \rangle \sim 0.6$ MeV. The neutrino-producing reactions which are at work inside the Sun are enumerated in the first column in Table 1. The second column in Table 1 shows abbreviation of these reactions. The energy spectrum of each reaction is shown in Fig. 1.

Observation of solar neutrinos directly addresses the theory of stellar structure and evolution, which is the basis of the standard solar model (SSM). The Sun as a well-defined neutrino source also provides extremely important opportunities to investigate nontrivial neutrino properties such as nonzero mass and mixing, because of the wide range of matter density and the great distance from the Sun to the Earth.

A pioneering solar neutrino experiment by Davis and collaborators using ^{37}Cl started in the late 1960's. From the very beginning of the solar-neutrino observation [1], it was recognized that the observed flux was significantly smaller than the SSM prediction, provided nothing happens to the electron neutrinos after they are created in the solar interior. This deficit has been called "the solar-neutrino problem."

In spite of the challenges by the chlorine and gallium radiochemical experiments (GALLEX, SAGE, and GNO) and water-Cherenkov experiments (Kamiokande and Super-Kamiokande), the solar-neutrino problem had persisted for more than 30

years. However, there have been remarkable developments in the past seven years. Thanks to the achievements of a heavy water Cherenkov experiment SNO and a reactor long baseline neutrino oscillation experiment KamLAND, the solar-neutrino problem has been finally solved.

In 2001, the initial result from SNO [2] on the solar-neutrino flux measured via charged-current (CC) reaction, $\nu_e d \to e^- pp$, combined with the Super-Kamiokande's high-statistics flux measurement via νe elastic scattering [3], provided direct evidence for flavor conversion of solar neutrinos [2]. Later in 2002, SNO's measurement of the neutral-current (NC) rate, $\nu d \to \nu pn$, and the updated CC result further strengthened this conclusion [4].

The most probable explanation which can also solve the solar-neutrino problem is neutrino oscillation. At this stage, the LMA (large mixing angle) solution was the most promising. However, at 3σ confidence level (CL), LOW (low probability or low mass) and/or VAC (vacuum) solutions were allowed depending on the method of analysis [5]. LMA and LOW are solutions of neutrino oscillation in matter [6,7] and VAC is a solution of neutrino oscillation in vacuum. Typical parameter values [5] corresponding to these solutions are

- LMA: $\Delta m^2 = 5.0 \times 10^{-5}$ eV^2, $\tan^2\theta = 0.42$
- LOW: $\Delta m^2 = 7.9 \times 10^{-8}$ eV^2, $\tan^2\theta = 0.61$
- VAC: $\Delta m^2 = 4.6 \times 10^{-10}$ eV^2, $\tan^2\theta = 1.8$.

It should be noted that all these solutions have large mixing angles. SMA (small mixing angle) solution (typical parameter values [5] are $\Delta m^2 = 5.0 \times 10^{-6}$ eV^2 and $\tan^2\theta = 1.5 \times 10^{-3}$) was once favored, but after SNO it was excluded at $> 3\sigma$ [5].

In December 2002, KamLAND observed clear evidence of neutrino oscillation with the allowed parameter region overlapping with the parameter region of the LMA solution [8]. Assuming CPT invariance, this result directly implies that the true solution of the solar ν_e oscillation has been determined to be LMA. A combined analysis of all the solar-neutrino data and KamLAND data significantly constrained the allowed parameter region. Inside the LMA region, the allowed region splits into two bands with lower Δm^2 ($\sim 7 \times 10^{-5}$ eV^2, called LMA I) and higher Δm^2 ($\sim 2 \times 10^{-4}$ eV^2, called LMA II).

In September, 2003, SNO reported [9] salt-phase results on solar-neutrino fluxes observed with NaCl added in heavy water: this improved the sensitivity for the detection of the NC reaction. A global analysis of all the solar neutrino data combined with the KamLAND data restricted the allowed parameter region to the LMA I region at greater than 99% CL.

Later, further results from KamLAND [10] significantly more constrained the allowed Δm^2 region. SNO also reported results from the complete salt phase [11]. A combined two-neutrino oscillation analysis [11] using the data from all solar-neutrino experiments and from KamLAND yields $\Delta m^2 = (8.0^{+0.6}_{-0.4}) \times 10^{-5}$ eV^2 and $\tan^2\theta = 0.45^{+0.09}_{-0.07}$ ($\theta = 33.9^{+2.4}_{-2.2}$ degrees).

Recently, a new solar neutrino experiment Borexino reported [12] the first realtime measurement of sub-MeV solar neutrinos with a low-background liquid scintillator detector. It is expected that Borexino as well as other low-energy solar neutrino experiments will further study properties of neutrinos and their interactions with matter on the one hand and the SSM on the other hand.

2. Solar Model Predictions

A standard solar model is based on the standard theory of stellar evolution. A variety of input information is needed in the evolutionary calculations. The most elaborate SSM calculations have been developped by Bahcall and his collaborators, who define their SSM as the solar model which is constructed with the best available physics and input data. Though they used no helioseismological constraints in defining the SSM, favorable models show an excellent agreement between the calculated and the helioseismologically-determined sound speeds to a precision of 0.1% rms throughout essentially the entire Sun. This greatly strengthens the confidence in the solar model. The currently preferred SSM is BS05(OP) developped by Bahcall and Serenelli [13,14]. This model uses newly calculated radiative opacities from the Opacity Project (OP) and previously standard heavy-element abundances (instead of the recently determined lower heavy-element abundances). However, BS05 (OP) [13] adopted conservative theoretical uncertainties in the solar-neutrino fluxes

in order to account for the differences between these two heavy-element abundance values. The BS05(OP) prediction [13] for the fluxes from neutrino-producing reactions is given in Table 1. The solar-neutrino spectra calculated with this model [13], is shown in Fig. 1. The event rates in chlorine and gallium solar-neutrino experiments are calculated by scaling the BP2000 SSM results [15] (see Table 1 in p. 460 of 2004 edition of Review of Particle Physics [16]) to the BS05(OP) fluxes, and are shown in Table 2. It should be noted, however, that Basu et al. have found [17] that models constructed with lower heavy-element abundances are incompatible with the observations of low-degree acoustic solar oscillation modes that probe the solar core. They therefore claim that the uncertainties in BS05(OP) predictions on the solar-neutrino fluxes (shown in Table 1) can be lowered.

Other recent solar-model prediction for solar-neutrino fluxes is given by Turck-Chièze *et al.* [18]. Their model, called a seismic model [19], is based on the standard theory of stellar evolution where the best physics available is adopted, but some fundamental inputs such as the *pp* reaction rate and the heavy-element abundances in the Sun are seismically adjusted within the commonly estimated errors aiming at reducing the residual differences between the helioseismologically-determined and the model-calculated sound speeds. Their prediction for the event rates in chlorine and gallium solar-neutrino experiments as well as ^{8}B solar-neutrino flux is shown in the last line in Table 2.

3. Solar Neutrino Experiments

So far, seven solar-neutrino experiments have published results. The most recent published results on the average event rates or flux from these experiments are listed in Table 2 and compared to the two recent solar-model predictions.

3.1. Radiochemical Experiments

Radiochemical experiments exploit electron neutrino absorption on nuclei followed by their decay through orbital electron capture. Produced Auger electrons are counted.

The Homestake chlorine experiment in USA uses the reaction

$$^{37}\mathrm{Cl} + \nu_e \rightarrow {}^{37}\mathrm{Ar} + e^- \ \text{(threshold 814 keV)}. \qquad (3)$$

Table 1: Neutrino-producing reactions in the Sun (first column) and their abbreviations (second column). The neutrino fluxes predicted by the BS05(OP) model [13] are listed in the third column. The theoretical errors of the neutrino fluxes are taken from "Historical (conservative)" errors given in Table 8 of Ref. [14].

Reaction	Abbr.	Flux ($\mathrm{cm}^{-2}\ \mathrm{s}^{-1}$)
$pp \to d\, e^+\, \nu$	*pp*	$5.99(1.00 \pm 0.01) \times 10^{10}$
$pe^-p \to d\, \nu$	*pep*	$1.42(1.00 \pm 0.02) \times 10^{8}$
$^3\mathrm{He}\ p \to {}^4\mathrm{He}\ e^+\nu$	*hep*	$7.93(1.00 \pm 0.16) \times 10^{3}$
$^7\mathrm{Be}\ e^- \to {}^7\mathrm{Li}\ \nu + (\gamma)$	^{7}Be	$4.84(1.00 \pm 0.11) \times 10^{9}$
$^8\mathrm{B} \to {}^8\mathrm{Be}^*\ e^+\nu$	^{8}B	$5.69(1.00 \pm 0.16) \times 10^{6}$
$^{13}\mathrm{N} \to {}^{13}\mathrm{C}\ e^+\nu$	^{13}N	$3.07(1.00^{+0.31}_{-0.28}) \times 10^{8}$
$^{15}\mathrm{O} \to {}^{15}\mathrm{N}\ e^+\nu$	^{15}O	$2.33(1.00^{+0.33}_{-0.29}) \times 10^{8}$
$^{17}\mathrm{F} \to {}^{17}\mathrm{O}\ e^+\nu$	^{17}F	$5.84(1.00 \pm 0.52) \times 10^{6}$

Three gallium experiments (GALLEX and GNO at Gran Sasso in Italy and SAGE at Baksan in Russia) use the reaction

$$^{71}\mathrm{Ga} + \nu_e \to {}^{71}\mathrm{Ge} + e^- \ \ (\text{threshold } 233 \text{ keV}). \qquad (4)$$

The produced ^{37}Ar and ^{71}Ge atoms are both radioactive, with half lives ($\tau_{1/2}$) of 34.8 days and 11.43 days, respectively. After an exposure of the detector for two to three times $\tau_{1/2}$, the reaction products are chemically extracted and introduced into a low-background proportional counter, where they are counted for a sufficiently long period to determine the exponentially decaying signal and a constant background.

Solar-model calculations predict that the dominant contribution in the chlorine experiment comes from ^{8}B neutrinos, but ^{7}Be, *pep*, ^{13}N, and ^{15}O neutrinos also contribute. At present, the most abundant *pp* neutrinos can be detected only in gallium experiments. Even so, according to the solar-model calculations, almost half of the capture rate in the gallium experiments is due to other solar neutrinos.

The Homestake chlorine experiment was the first to attempt the observation of solar neutrinos. Initial results obtained in 1968 showed no events above background with upper limit

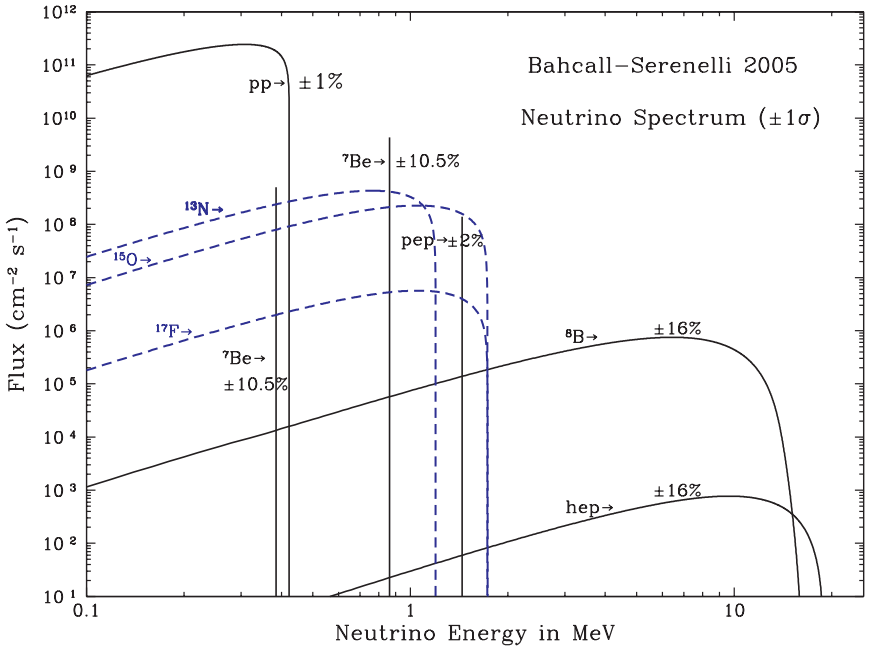

Figure 1: The solar neutrino spectrum predicted by the BS05(OP) standard solar model [13]. The neutrino fluxes from continuum sources are given in units of number $\mathrm{cm}^{-2}\mathrm{s}^{-1}\mathrm{MeV}^{-1}$ at one astronomical unit, and the line fluxes are given in number $\mathrm{cm}^{-2}\mathrm{s}^{-1}$.

for the solar-neutrino flux of 3 SNU [1]. After introduction of an improved electronics system which discriminates signal from background by measuring the rise time of the pulses from proportional counters, a finite solar-neutrino flux has been observed since 1970. The solar-neutrino capture rate shown in Table 2 is a combined result of 108 runs between 1970 and 1994 [20]. It is only about 1/3 of the solar-model predictions [13, 18].

GALLEX presented the first evidence of *pp* solar-neutrino observation in 1992 [26]. Here also, the observed capture rate is significantly less than the SSM prediction. SAGE initially reported very low capture rate, $20^{+15}_{-20} \pm 32$ SNU, with a 90% confidence-level upper limit of 79 SNU [27]. Later, SAGE [28] observed similar capture rate to that of GALLEX. Both GALLEX and SAGE groups tested the overall detector

Table 2: Results from the seven solar-neutrino experiments. Recent solar model calculations are also presented. The first and the second errors in the experimental results are the statistical and systematic errors, respectively. SNU (Solar Neutrino Unit) is defined as 10^{-36} neutrino captures per atom per second.

	$^{37}\mathrm{Cl}\rightarrow{}^{37}\mathrm{Ar}$ (SNU)	$^{71}\mathrm{Ga}\rightarrow{}^{71}\mathrm{Ge}$ (SNU)	$^{8}\mathrm{B}$ ν flux ($10^{6}\mathrm{cm}^{-2}\mathrm{s}^{-1}$)
Homestake			
(CLEVELAND 98)[20]	$2.56 \pm 0.16 \pm 0.16$	—	—
GALLEX			
(HAMPEL 99)[21]	—	$77.5 \pm 6.2^{+4.3}_{-4.7}$	—
GNO			
(ALTMANN 05)[22]	—	$62.9^{+5.5}_{-5.3} \pm 2.5$	—
GNO+GALLEX			
(ALTMANN 05)[22]	—	$69.3 \pm 4.1 \pm 3.6$	—
SAGE			
(ABDURASHI...02)[23]	—	$70.8^{+5.3+3.7}_{-5.2-3.2}$	—
Kamiokande			
(FUKUDA 96)[24]	—	—	$2.80 \pm 0.19 \pm 0.33^{\dagger}$
Super-Kamiokande			
(HOSAKA 05)[25]	—	—	$2.35 \pm 0.02 \pm 0.08^{\dagger}$
SNO (pure D_2O)			
(AHMAD 02)[4]	—	—	$1.76^{+0.06}_{-0.05} \pm 0.09^{\ddagger}$
	—	—	$2.39^{+0.24}_{-0.23} \pm 0.12^{\dagger}$
	—	—	$5.09^{+0.44+0.46*}_{-0.43-0.43}$
SNO (NaCl in D_2O)			
(AHARMIM 05)[11]	—	—	$1.68 \pm 0.06^{+0.08\ddagger}_{-0.09}$
	—	—	$2.35 \pm 0.22 \pm 0.15^{\dagger}$
	—	—	$4.94 \pm 0.21^{+0.38*}_{-0.34}$
BS05(OP) SSM [13]	8.1 ± 1.3	126 ± 10	$5.69(1.00 \pm 0.16)$
Seismic model [18]	7.64 ± 1.1	123.4 ± 8.2	5.31 ± 0.6

* Flux measured via the neutral-current reaction.

† Flux measured via νe elastic scattering.

‡ Flux measured via the charged-current reaction.

response with intense man-made ^{51}Cr neutrino sources, and observed good agreement between the measured ^{71}Ge production rate and that predicted from the source activity, demonstrating

the reliability of these experiments. The GALLEX Collaboration formally finished observations in early 1997. Since April, 1998, a newly defined collaboration, GNO (Gallium Neutrino Observatory) continued the observations until April 2003. The complete GNO results are published in Ref. [22]. The GNO + GALLEX joint analysis results are also presented [22] (see Table 2).

3.2 Kamiokande and Super-Kamiokande

Kamiokande and Super-Kamiokande in Japan are real-time experiments utilizing νe scattering

$$\nu_x + e^- \rightarrow \nu_x + e^- \tag{5}$$

in a large water-Cherenkov detector. It should be noted that the reaction Eq. (5) is sensitive to all active neutrinos, $x = e$, μ, and τ. However, the sensitivity to ν_μ and ν_τ is much smaller than the sensitivity to ν_e, $\sigma(\nu_{\mu,\tau}e) \approx 0.16\,\sigma(\nu_e e)$. The solar-neutrino flux measured via νe scattering is deduced assuming no neutrino oscillations.

These experiments take advantage of the directional correlation between the incoming neutrino and the recoil electron. This feature greatly helps the clear separation of the solar-neutrino signal from the background. Due to the high thresholds (7 MeV in Kamiokande and 5 MeV at present in Super-Kamiokande) the experiments observe pure ^{8}B solar neutrinos because *hep* neutrinos contribute negligibly according to the SSM.

The Kamiokande-II Collaboration started observing ^{8}B solar neutrinos at the beginning of 1987. Because of the strong directional correlation of νe scattering, this result gave the first direct evidence that the Sun emits neutrinos [29] (no directional information is available in radiochemical solar-neutrino experiments). The observed solar-neutrino flux was also significantly less than the SSM prediction. In addition, Kamiokande-II obtained the energy spectrum of recoil electrons and the fluxes separately measured in the daytime and nighttime. The Kamiokande-II experiment came to an end at the beginning of 1995.

Super-Kamiokande is a 50-kton second-generation solar-neutrino detector, which is characterized by a significantly

larger counting rate than the first-generation experiments. This experiment started observation in April 1996. In November 2001, Super-Kamiokande suffered from an accident in which substantial number of photomultiplier tubes were lost. The detector was rebuilt within a year with about half of the original number of photomultiplier tubes. The experiment with the detector before the accident is called Super-Kamiokande-I, and that after the accident is called Super-Kamiokande-II. The complete Super-Kamiokande-I solar-neutrino results are reported in Ref. [25]. The solar-neutrino flux is measured as a function of zenith angle and recoil-electron energy. The average solar-neutrino flux is given in Table 2. The observed day-night asymmetry is $A_{\rm DN} = \dfrac{\rm Day - Night}{0.5({\rm Day + Night})} = -0.021 \pm 0.020^{+0.013}_{-0.012}$. No indication of spectral distortion is observed.

3.3 SNO

In 1999, a new real time solar-neutrino experiment, SNO, in Canada started observation. This experiment uses 1000 tons of ultra-pure heavy water (D_2O) contained in a spherical acrylic vessel, surrounded by an ultra-pure H_2O shield. SNO measures ^{8}B solar neutrinos via the reactions

$$\nu_e + d \rightarrow e^- + p + p \tag{6}$$

and

$$\nu_x + d \rightarrow \nu_x + p + n, \tag{7}$$

as well as νe scattering, Eq. (5). The CC reaction, Eq. (6), is sensitive only to electron neutrinos, while the NC reaction, Eq. (7), is sensitive to all active neutrinos.

The Q-value of the CC reaction is -1.4 MeV and the electron energy is strongly correlated with the neutrino energy. Thus, the CC reaction provides an accurate measure of the shape of the ^{8}B solar-neutrino spectrum. The contributions from the CC reaction and νe scattering can be distinguished by using different $\cos\theta_\odot$ distributions where $\theta_\odot$ is the angle of the electron momentum with respect to the direction from the Sun to the Earth. While the νe scattering events have a strong forward peak, CC events have an approximate angular distribution of $1 - 1/3\ \cos\theta_\odot$.

The threshold of the NC reaction is 2.2 MeV. In the pure D_2O, the signal of the NC reaction is neutron capture in deuterium, producing a 6.25-MeV γ-ray. In this case, the capture efficiency is low and the deposited energy is close to the detection threshold of 5 MeV. In order to enhance both the capture efficiency and the total γ-ray energy (8.6 MeV), 2 tons of NaCl were added to the heavy water in the second phase of the experiment. In addition, discrete ^{3}He neutron counters were installed and the NC measurement with them are being made as the third phase of the SNO experiment.

In 2001, SNO published the initial results on the measurement of the ^{8}B solar-neutrino flux via CC reaction [2]. The electron energy spectrum and the $\cos\theta_\odot$ distribution were also measured. The spectral shape of the electron energy was consistent with the expectations for an undistorted ^{8}B solar-neutrino spectrum.

SNO also measured the ^{8}B solar-neutrino flux via νe scattering [2]. Though the latter result had poor statistics, it was consistent with the high-statistics Super-Kamiokande result. Thus, the SNO group compared their CC result with Super-Kamiokande's νe scattering result, and obtained evidence of an active non-ν_e component in the solar-neutrino flux [2], as further described in Sec. 3.5.

Later, in April, 2002, SNO reported the first result on the ^{8}B solar-neutrino flux measurement via NC reaction [4]. The total flux measured via NC reaction was consistent with the solar-model predictions (see Table 2). Also, the SNO's CC and νe scattering results were updated [4]. These results were consistent with the earlier results [2].

The SNO Collaboration made a global analysis (see Sect. 3.6) of the SNO's day and night energy spectra together with the data from other solar-neutrino experiments. The results strongly favored the LMA solution, with the LOW solution allowed at 99.5% CL [30]. (In most of the similar global analyses, the VAC solution was also allowed at $99.9 \sim 99.73\%$ CL [5]) .

In September, 2003, SNO has released the first results of solar-neutrino flux measurements with dissolved NaCl in

the heavy water [9]. The complete salt phase results are also reported recently [11]. Using the salt phase results, the SNO Collaboration made a global solar-neutrino analysis and a global solar + KamLAND analysis. Implications of these analyses are described in Sect. 5.

SNO also studied the energy spectrum and day-night flux asymmetries for both pure D_2O [30] and salt phases [11]. The energy spectrum deduced from the CC reaction is consistent with the spectrum expected from an undistorted ^{8}B spectral shape. No significant day-night flux asymmetries are observed within uncertainties. These observations are consistent with the best-fit LMA solution from the global solar + KamLAND analysis.

3.4 Comparison of Experimental Results with Solar-Model Predictions

It is clearly seen from Table 2 that the results from all the solar-neutrino experiments, except the SNO's NC result, indicate significantly less flux than expected from the solar-model predictions [13, 18].

There has been a consensus that a consistent explanation of all the results of solar-neutrino observations is unlikely within the framework of astrophysics using the solar-neutrino spectra given by the standard electroweak model. Many authors made solar model-independent analyses constrained by the observed solar luminosity [31–35], where they attempted to fit the measured solar-neutrino capture rates and ^{8}B flux with normalization-free, undistorted energy spectra. All these attempts only obtained solutions with very low probabilities.

The data therefore suggest that the solution to the solar-neutrino problem requires nontrivial neutrino properties.

3.5 Evidence for Solar Neutrino Oscillations

Denoting the ^{8}B solar-neutrino flux obtained by the SNO's CC measurement as $\phi^{\rm CC}_{\rm SNO}(\nu_e)$ and that obtained by the Super-Kamiokande νe scattering as $\phi^{\rm ES}_{\rm SK}(\nu_x)$, $\phi^{\rm CC}_{\rm SNO}(\nu_e) = \phi^{\rm ES}_{\rm SK}(\nu_x)$ is expected for the standard neutrino physics. However, SNO's initial data [2] indicated

$$\phi^{\rm ES}_{\rm SK}(\nu_x) - \phi^{\rm CC}_{\rm SNO}(\nu_e) = (0.57 \pm 0.17) \times 10^6 \ {\rm cm}^{-2}{\rm s}^{-1}. \qquad (8)$$

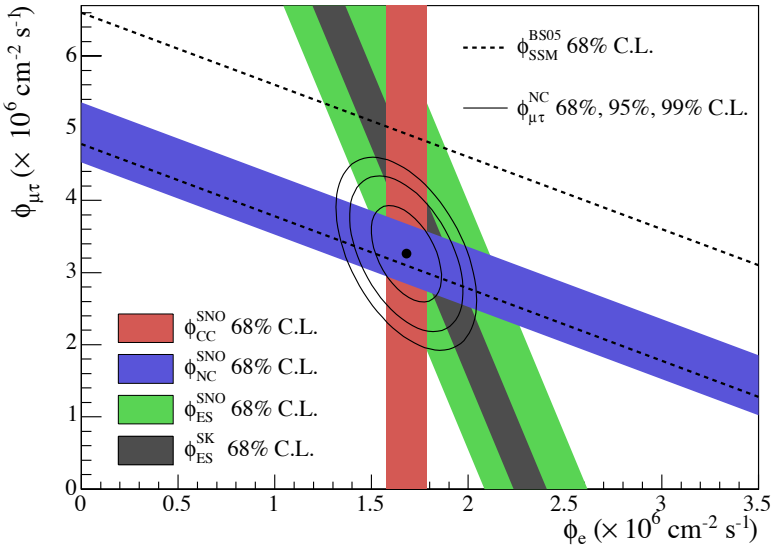

Figure 2: Fluxes of ^{8}B solar neutrinos, $\phi(\nu_e)$, and $\phi(\nu_{\mu \text{ or } \tau})$, deduced from the SNO's charged-current (CC), ν_e elastic scattering (ES), and neutral-current (NC) results for the salt phase measurement [11]. The Super-Kamiokande ES flux is from Ref. [36]. The BS05(OP) standard solar model prediction [13] is also shown. The bands represent the 1σ error. The contours show the 68%, 95%, and 99% joint probability for $\phi(\nu_e)$ and $\phi(\nu_{\mu \text{ or } \tau})$. This figure is taken from Ref. [11]. Color version at end of book.

The significance of the difference was $> 3\sigma$, implying direct evidence for the existence of a non-ν_e active neutrino flavor component in the solar-neutrino flux. A natural and most probable explanation of neutrino flavor conversion is neutrino oscillation. Note that both the SNO [2] and Super-Kamiokande [3] flux results were obtained by assuming the standard ^{8}B neutrino spectrum shape. This assumption was justified by the measured energy spectra in both experiments.

The SNO's results for the pure D_2O phase, reported in 2002 [4], provided stronger evidence for neutrino oscillation than Eq. (8). The fluxes measured with CC, ES, and NC events

were deduced. Here, the spectral distributions of the CC and ES events were constrained to an undistorted ^{8}B shape. The results are

$$\phi_{\rm SNO}^{\rm CC}(\nu_e) = (1.76^{+0.06}_{-0.05} \pm 0.09) \times 10^6 {\rm cm}^{-2}{\rm s}^{-1} \ , \qquad (9)$$

$$\phi_{\rm SNO}^{\rm ES}(\nu_x) = (2.39^{+0.24}_{-0.23} \pm 0.12) \times 10^6 {\rm cm}^{-2}{\rm s}^{-1} \ , \qquad (10)$$

$$\phi_{\rm SNO}^{\rm NC}(\nu_x) = (5.09^{+0.44+0.46}_{-0.43-0.43}) \times 10^6 {\rm cm}^{-2}{\rm s}^{-1} \ . \qquad (11)$$

Eq. (11) is a mixing-independent result and therefore tests solar models. It shows good agreement with the ^{8}B solar-neutrino flux predicted by the solar models [13, 18]. The flux of non-ν_e active neutrinos, $\phi(\nu_{\mu \text{ or } \tau})$, can be deduced from these results. It is

$$\phi(\nu_{\mu \text{ or } \tau}) = \left(3.41^{+0.66}_{-0.64}\right) \times 10^6 {\rm cm}^{-2}{\rm s}^{-1} \qquad (12)$$

where the statistical and systematic errors are added in quadrature. This $\phi(\nu_{\mu \text{ or } \tau})$ is 5.3 σ above 0. The non-zero $\phi(\nu_{\mu \text{ or } \tau})$ is strong evidence for neutrino flavor transformation.

From the salt phase measurement [11], the fluxes measured with CC and ES events were deduced with no constraint of the ^{8}B energy spectrum. The results are

$$\phi_{\rm SNO}^{\rm CC}(\nu_e) = (1.68 \pm 0.06^{+0.08}_{-0.09}) \times 10^6 {\rm cm}^{-2}{\rm s}^{-1} \ , \qquad (13)$$

$$\phi_{\rm SNO}^{\rm ES}(\nu_x) = (2.35 \pm 0.22 \pm 0.15) \times 10^6 {\rm cm}^{-2}{\rm s}^{-1} \ , \qquad (14)$$

$$\phi_{\rm SNO}^{\rm NC}(\nu_x) = (4.94 \pm 0.21^{+0.38}_{-0.34}) \times 10^6 {\rm cm}^{-2}{\rm s}^{-1} \ . \qquad (15)$$

These results are consistent with the results from the pure D_2O phase. Fig. 2 shows the salt phase result of $\phi(\nu_{\mu \text{ or } \tau})$ versus the flux of electron neutrinos $\phi(\nu_e)$ with the 68%, 95%, and 99% joint probability contours.

4. KamLAND Reactor Neutrino Oscillation Experiment

KamLAND is a 1-kton ultra-pure liquid scintillator detector located at the old Kamiokande's site in Japan. Although the ultimate goal of KamLAND is observation of ^{7}Be solar neutrinos with much lower energy threshold, the initial phase of the experiment is a long baseline (flux-weighted average distance of $\sim$ 180 km) neutrino oscillation experiment using $\bar{\nu}_e$'s emitted from power reactors. The reaction $\bar{\nu}_e + p \rightarrow e^+ + n$ is used

to detect reactor $\bar{\nu}_e$'s and delayed coincidence with 2.2 MeV γ-ray from neutron capture on a proton is used to reduce the backgrounds.

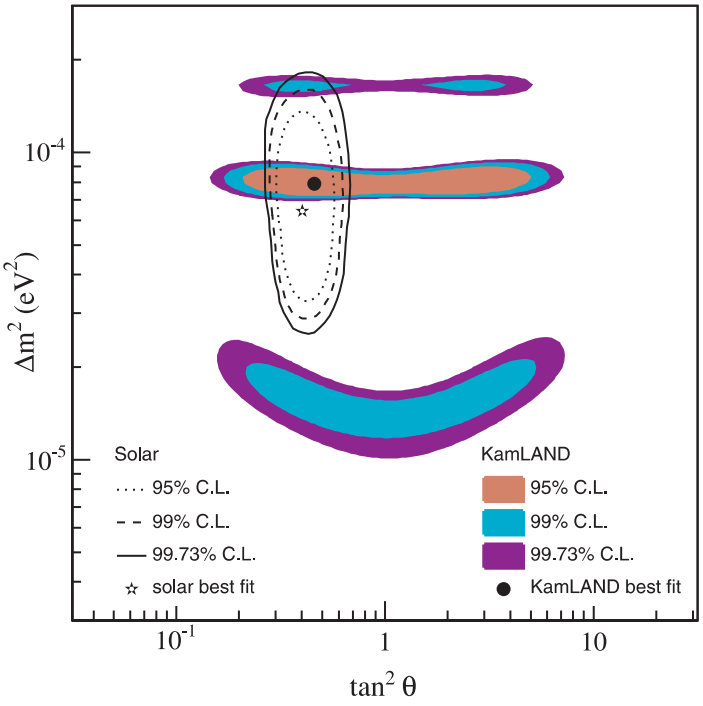

Figure 3: Allowed regions of neutrino-oscillation parameters from the KamLAND 766 ton·yr exposure $\bar{\nu}_e$ data [10]. The LMA region from solar-neutrino experiments [9] is also shown. This figure is taken from Ref. [10]. Color version at end of book.

With the reactor $\bar{\nu}_e$'s energy spectrum (< 8 MeV) and a prompt-energy analysis threshold of 2.6 MeV, this experiment has a sensitive Δm^2 range down to $\sim 10^{-5}$ eV^2. Therefore, if the LMA solution is the real solution of the solar neutrino problem, KamLAND should observe reactor $\bar{\nu}_e$ disappearance, assuming CPT invariance.

The first KamLAND results [8] with 162 ton·yr exposure were reported in December 2002. The ratio of observed to

expected (assuming no neutrino oscillation) number of events was

$$\frac{N_{\rm obs} - N_{\rm BG}}{N_{\rm NoOsc}} = 0.611 \pm 0.085 \pm 0.041. \qquad (16)$$

with obvious notation. This result shows clear evidence of event deficit expected from neutrino oscillation. The 95% CL allowed regions are obtained from the oscillation analysis with the observed event rates and positron spectrum shape. There are two bands of regions allowed by both solar and KamLAND data in the region. The LOW and VAC solutions are excluded by the KamLAND results. A combined global solar + KamLAND analysis showed that the LMA is a unique solution to the solar neutrino problem with $> 5\sigma$ CL [37].

In June 2004, KamLAND released the results from 766 ton·yr exposure [10]. In addition to the deficit of events, the observed positron spectrum showed the distortion expected from neutrino oscillation. Fig. 3 shows the allowed regions in the neutrino-oscillation parameter space. The best-fit point lies in the region called LMA I. The LMA II region is disfavored at the 98% CL.

5. Global Neutrino Oscillation Analysis

The SNO Collaboration updated [11] a global two-neutrino oscillation analysis of the solar-neutrino data including the SNO's complete salt phase data, and global solar + KamLAND 766 ton·yr data [10]. The resulting neutrino oscillation contours are shown in Fig. 4. The best fit parameters for the global solar analysis are $\Delta m^2 = 6.5^{+4.4}_{-2.3} \times 10^{-5}$ eV^2 and $\tan^2\theta = 0.45^{+0.09}_{-0.08}$. The inclusion of the KamLAND data significantly constrains the allowed Δm^2 region, but shifts the best-fit Δm^2 value. The best-fit parameters for the global solar + KamLAND analysis are $\Delta m^2 = 8.0^{+0.6}_{-0.4} \times 10^{-5}$ eV^2 and $\tan^2\theta = 0.45^{+0.09}_{-0.07}$ ($\theta = 33.9^{+2.4}_{-2.2}$).

A number of authors [38 - 40] also made combined global neutrino oscillation analysis of solar + KamLAND data in mostly three-neutrino oscillation framework using the SNO complete salt phase data [11] and the KamLAND 766 ton·yr data [10]. These give consistent results with the SNO's two-neutrino oscillation analysis [11].

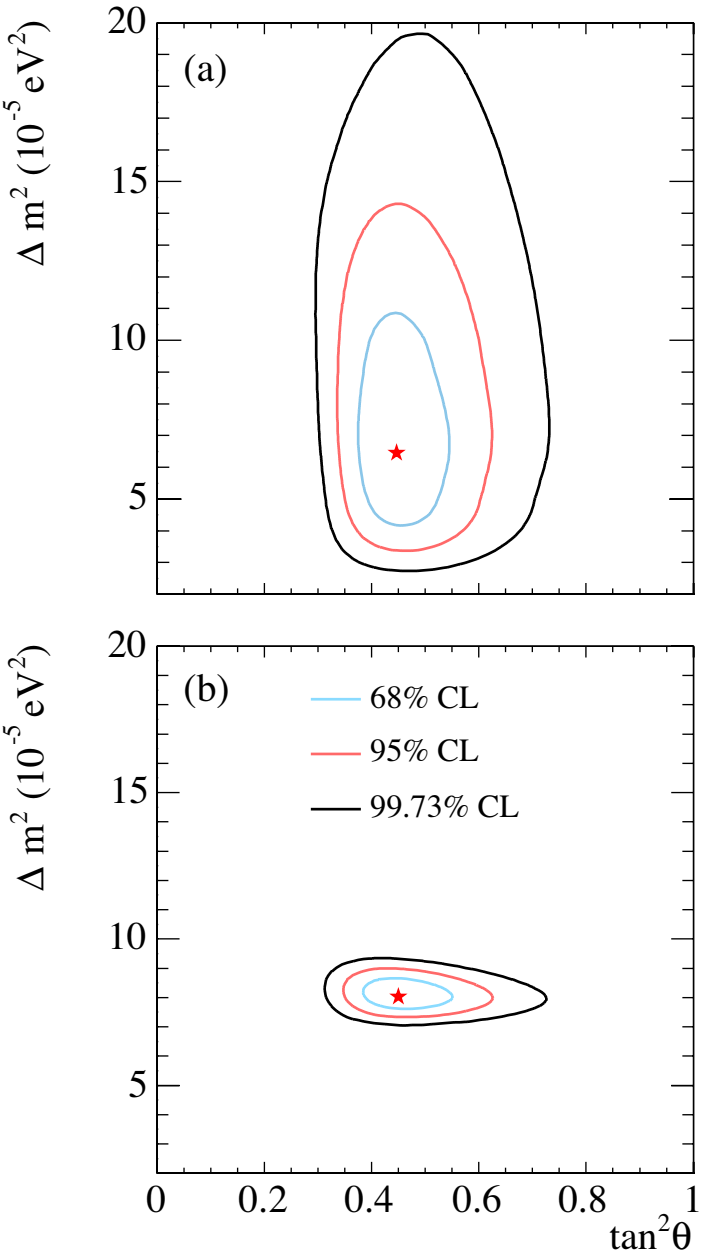

Figure 4: Update of the global neutrino oscillation contours given by the SNO Collaboration assuming that the ^{8}B neutrino flux is free and the *hep* neutrino flux is fixed. (a) Solar global analysis. (b) Solar global + KamLAND. This figure is taken from Ref. [11].

6. Recent Progress and Future Prospects

Now that the solar-neutrino problem has been essentially solved, what are the future prospects of the solar-neutrino experiments?

From the particle-physics point of view, precise determination of the oscillation parameters and search for non-standard physics such as a small admixture of a sterile component in the solar-neutrino flux will be still of interest. More precise NC measurements by SNO will contribute in reducing the uncertainty of the mixing angle [41]. Measurements of the pp flux to an accuracy comparable to the quoted accuracy ($\pm 1\%$) of the SSM calculation will significantly improve the precision of the mixing angle [42,43].

An important task of the future solar neutrino experiments is further tests of the SSM by measuring monochromatic ^{7}Be neutrinos and fundamental *pp* neutrinos. The ^{7}Be neutrino flux will be measured by a new experiment, Borexino, at Gran Sasso via νe scattering in 300 tons of ultra-pure liquid scintillator with a detection threshold as low as 250 keV. KamLAND will also observe ^{7}Be neutrinos if the detection threshold can be lowered to a level similar to that of Borexino.

Borexino has recently reported the first realtime observation of monochromatic 0.862 MeV ^{7}Be solar neutrinos [12]. With 47.4 live days, the observed rate, $47 \pm 7 \pm 12$ counts/(100 ton·day), is consistent with the rate calculated with SSM and neutrino oscillations, 49 ± 4 counts/(100 ton·day). For comparison, the expected rate with no neutrino oscillations is 75 ± 4 counts/(100 ton·day).

For the detection of *pp* neutrinos, various ideas for the detection scheme have been presented. However, no experiments have been approved yet, and extensive R&D efforts are still needed for any of these ideas to prove its feasibility.

References

1. D. Davis, Jr., D.S. Harmer, and K.C. Hoffman, Phys. Rev. Lett. **20**, 1205 (1968).
2. Q.R. Ahmad *et al.*, Phys. Rev. Lett. **87**, 071301 (2001).
3. Y. Fukuda *et al.*, Phys. Rev. Lett. **86**, 5651 (2001).
4. Q.R. Ahmad *et al.*, Phys. Rev. Lett. **89**, 011301 (2002).

5. See, for example, J.N. Bahcall, C.M. Gonzalez-Garcia, and C. Peña-Garay, JHEP 0207, 054 (2002).
6. L. Wolfenstein, Phys. Rev. **D17**, 2369 (1978).
7. S.P. Mikheyev and A. Yu. Smirnov, Sov. J. Nucl. Phys. **42**, 913 (1985).
8. K. Eguchi *et al.*, Phys. Rev. Lett. **90**, 021802 (2003).
9. S.N. Ahmed *et al.*, Phys. Rev. Lett. **92**, 181301 (2004).
10. T. Araki *et al.*, Phys. Rev. Lett. **94**, 081801 (2005).
11. B. Aharmim *et al.*, Phys. Rev. **C72**, 055502 (2005).
12. C. Arpesella *et al.*, Phys. Lett. **B658**, 101 (2008).
13. J.N. Bahcall, A.M. Serenelli, and S. Basu, Astrophys. J. **621**, L85 (2005).
14. J.N. Bahcall and A.M. Serenelli Astrophys. J. **626**, 530 (2005).
15. J.N. Bahcall, M.H. Pinsonneault, and S. Basu, Astrophys. J. **555**, 990 (2001).
16. S. Eidelman *et al.*, Phys. Lett. **B592**, 1 (2004).
17. S. Basu *et al.*, Astrophys. J. **655**, 660 (2007).
18. S. Turck-Chièze *et al.*, Phys. Rev. Lett. **93**, 211102 (2004).
19. S. Couvidat, S. Turck-Chièze, and A.G. Kosovichev, Astrophys. J. **599**, 1434 (2003).
20. B.T. Cleveland *et al.*, Ap. J. **496**, 505 (1998).
21. W. Hampel *et al.*, Phys. Lett. **B447**, 127 (1999).
22. M. Altmann *et al.*, Phys. Lett. **B616**, 174 (2005).
23. J.N. Abdurashitov *et al.*, Sov. Phys. JETP **95**, 181 (2002).
24. Y. Fukuda *et al.*, Phys. Rev. Lett. **77**, 1683 (1996).
25. J. Hosaka *et al.*, Phys. Rev. **D73**, 112001 (2006).
26. P. Anselmann *et al.*, Phys. Lett. **B285**, 376 (1992).
27. A.I. Abazov *et al.*, Phys. Rev. Lett. **67**, 3332 (1991).
28. J.N. Abdurashitov *et al.*, Phys. Lett. **B328**, 234 (1994).
29. K.S. Hirata *et al.*, Phys. Rev. Lett. **63**, 16 (1989).
30. Q.R. Ahmad *et al.*, Phys. Rev. Lett. **89**, 011302 (2002).
31. N. Hata, S. Bludman, and P. Langacker, Phys. Rev. **D49**, 3622 (1994).
32. N. Hata and P. Langacker, Phys. Rev. **D52**, 420 (1995).
33. N. Hata and P. Langacker, Phys. Rev. **D56**, 6107 (1997).
34. S. Parke, Phys. Rev. Lett. **74**, 839 (1995).
35. K.M. Heeger and R.G.H. Robertson, Phys. Rev. Lett. **77**, 3720 (1996).
36. Y. Fukuda *et al.*, Phys. Lett. **B539**, 179 (2002).

37. See, for example, J.N. Bahcall, M.C. Gonzalez-Garcia, and C. Peña-Garay, JHEP 0302, 009 (2003).
38. A.B. Balantekin *et al.*, Phys. Lett. **B613**, 61 (2005).
39. A. Strumia and F. Vissani, Nucl. Phys. **B726**, 294 (2005).
40. G.L. Fogli *et al.*, Prog. Part. Nucl. Phys. **57**, 742 (2006).
41. A. Bandyopadhyay *et al.*, Phys. Lett. **B608**, 115 (2005).
42. J.N. Bahcall and C. Peña-Garay, JHEP 0311, 004 (2003).
43. A. Bandyopadhyay *et al.*, Phys. Rev. **D72**, 033013 (2005).